

## CHAPTER 7

## FABRICATION, SPECTRAL RESPONSE AND FLAT BAND POTENTIAL

## MEASUREMENTS OF PEC SOLAR CELLS USING

 $\text{MoSe}_x\text{Te}_{2-x}$  SINGLE CRYSTALS

	CONTENTS	PAGES
7.1	Introduction	126
7.2	Fabrication of PEC solar cells	127
7.3	Results and discussion	127
7.3.1	Spectral response measurements	127
7.3.2	Capacitance measurements	129
7.4	Conclusions	133
	References	135
	Figures	

## 7.1 Introduction

Since the energy conversion efficiency of a solar cell device depends upon the optical band gap of semiconducting material and better energy conversion efficiency is obtained when the optical band lies in the range 1.1 to 2.1 eV<sup>1-5</sup>). Various workers<sup>6-10</sup>) have attempted the preparation of solid solutions of two compounds and used them as photoelectrode materials. In general, the properties like band gap energy, band positions of a solid solution is dependent on its composition and is intermediate between that of the two components. Thus the suitable band gap material can be easily made available from appropriate composition of constituents. The importance of transition metal dichalcogenides as solar energy materials for efficient conversion of light energy to electrical or chemical energy has already been explained earlier. These materials form a wide range of solid solutions with either mixed metal or chalcogenide composition or both keeping this in view, author has made attempts to fabricate the photoelectrochemical solar cells using the grown crystals of  $\text{MoSe}_x\text{Te}_{2-x}$  ( $0 \leq x \leq 2$ ) and characterize them optically and

electrochemically. Determination of optical band gap from spectral responses and flat band potentials in the present work on  $\text{MoSe}_x\text{Te}_{2-x}$  have been made by capacitance measurements from Mott-Schottky plots.

## 7.2 Fabrication of PEC Solar Cells

A glass tube with a uniform bore and flattened end was used for mounting the single crystals. Copper wire was introduced through the bore and connected to the crystal using silver paste. The electrode surface was insulated at the edges using a good epoxy. The semiconductor electrode was then immersed in an aqueous Iodine/Iodide electrolyte prepared by mixing 5.0 M NaI, 0.01 M  $\text{I}_2$  and 0.5 M  $\text{Na}_2\text{SO}_4$  in double distilled water and platinum grid as counter electrode.

## 7.3 Results and Discussion

### 7.3.1 Spectral Response Measurements

The experimental arrangement for the spectral response measurement of PEC cell is shown in Fig. 7.1. The arrangement consists of a grating

monochromator ( CEL, India), PEC cell using  $\text{MoSe}_x\text{Te}_{2-x}$  electrode and digital multimeter. The PEC cell has been illuminated by monochromatic light from a monochromator and spectral response has been observed for wavelengths 910 nm to 500 nm at an interval of 10 nm.

The semiconductor electrode interface can be treated as Schottky barrier<sup>3)</sup> and the photocurrent has the following behaviour

$$J = e\phi_0 \left\{ 1 - \frac{\exp [-\alpha W_0 (V - V_{fb})^{1/2}]}{1 - L_P} \right\} \quad (7.1)$$

where  $\phi_0$  is the photon flux,

$L_P$  is the hole diffusion length,

$V_{fb}$  is the flat band potential,

$\alpha$  is the optical absorption coefficient and

$W_0$  is characteristic depletion width.

$W_0$  is given by  $(2\epsilon / e N_D)^{1/2}$

where  $\epsilon$  is the dielectric constant,  $e$  is the electronic charge and  $N_D$  the donor density.

It has been shown that the optical absorption for interband transitions in a semiconductor close to the gap behaves as

$$\alpha = \frac{A (h\nu - E_g)^{n/2}}{h\nu} \quad (7.2)$$

where  $n = 1$  for direct and  $n = 4$  for indirect transitions. These two equations completely describe the photoresponse of semiconductor-electrolyte junction.

It has been suggested by Lemasson et al.<sup>11)</sup> that the photoresponse is directly proportional to the photon flux and by Redon and Vigneron<sup>12)</sup> that the photocurrent is proportional to absorption spectrum. The plots of  $(Jh\nu)^2$  versus  $h\nu$  (Fig. 7.2) for the compounds of  $\text{MoSe}_x\text{Te}_{2-x}$ , are straight lines ( $n = 1$ ) indicating that these materials are direct band gap semiconductors. The values of optical band gaps obtained

from  $(Jh\nu)^2$  versus  $h\nu$  plots (Fig. 7.2) are given in Table 7.1. It has been observed that the band gaps of  $\text{MoSe}_2\text{Te}_{2-x}$  increase from 1.1 eV for  $\text{MoTe}_2$  to 1.4 eV for  $\text{MoSe}_2$ .

### 7.3.2 Capacitance Measurements

The semiconductor-electrolyte interface can be treated as two capacitances in series, one in the electrolyte near the surface (Helmoltz layer)  $C_H$ , and the other capacitor formed in the semiconductor by the depletion region  $C_{SC}^{(4)}$ . Since these two capacitors are in series and  $C_{SC} \ll C_H$ , the net capacitance is very close to  $C_{SC}$ . According to depletion layer approximation the capacitance of space charge layer varies with the bias applied to the semiconductor by the Mott-Schottky relation<sup>5,6)</sup>

$$\frac{1}{C_{SC}^2} = \frac{2}{\epsilon \epsilon_0 e N_D} \left( |V_{SCE}| - \frac{kT}{e} \right) \quad (7.3)$$

where  $\epsilon$  is the dielectric constant,  
 $\epsilon_0$  is the permittivity of free space,  
 $e$  is the charge of electron,

Table 7.1

The Values of opticalband gap and donor concentrations  
in  $\text{MoSe}_x\text{Te}_{2-x}$  ( $0 \leq x \leq 2$ )

Composition	Band gap (eV)	Donor concentration $N_D$ ( $\text{cm}^{-3}$ )	$E_C - E_F$ (versus SCE) (V)
$\text{MoSe}_2$	1.40	$1.56 \times 10^{16}$	0.164
$\text{MoSe}_{1.5}\text{Te}_{0.5}$	1.29	$0.87 \times 10^{16}$	0.179
$\text{MoSeTe}$	1.24	$1.22 \times 10^{16}$	0.170
$\text{MoSe}_{0.5}\text{Te}_{1.5}$	1.16	$3.8 \times 10^{16}$	0.140
$\text{MoTe}_2$	1.10	$6.1 \times 10^{16}$	0.129

$N_D$  donor concentration,

$V_{SCE}$  applied potential across the space charge layer which can be expressed as  $V_{SCE} = V - V_{fb}$ ,

$V_{fb}$  is the flat band potential. Fer

From equation (7.3) it is seen that the straight line would be obtained if  $1 / C_{SC}^2$  versus  $V$  is plotted. This is termed as Mott-Schottky plot. The  $s$  intercept on the  $V$  axis gives the flat band potential  $V_{fb}$  and from the slope of the curve the value of the donor concentration  $N_D$  can be calculated.

Mott-Schottky plots of  $MoSe_xTe_{2-x}$  ( $0 \leq x \leq 2$ ) electrodes are depicted in Fig. 7.3. The flat band potentials evaluated are found to be increasing from  $V_{SCE} = 0.325$  V for  $MoSe_2$  to  $-0.2$  V for  $MoTe_2$ . The variation of flat band potential with the composition of  $MoSe_2Te_{2-x}$  single crystals is shown in Fig. 7.4. The donor concentrations  $N_D$  have been determined from the slope of Mott-Schottky relation as ,

$$N_D = 2 \left[ e \epsilon \epsilon_0 (\text{slope}) \right]^{-1} \quad (7.4)$$



The donor concentrations calculated using the above relation are shown in Table 7.1.

The distance between the conduction band minimum  $E_C$  and flat band potential  $V_{fb}$  is important to localise the valence band maximum.

According to Kautek and Gerischer<sup>13)</sup> in classical approximation where  $(E_C - E_{fb})/kT > 1$ , the effective density of conduction states is given by

$$N_C = \frac{2}{h^3} (2 \pi m_e^* k T)^{3/2} \quad (7.5)$$

$m_e^*$  is the effective mass of electron and is taken to be  $0.15 m_e^{14)$ ,  $m_e$  mass of electron for transition metal dichalcogenides  $N_C$  comes out to be  $8.8 \times 10^{18} \text{ cm}^{-3}$ . Assuming that all donors are ionised and have given their electrons into the conduction band, we get the classical Maxwell Boltzmann distribution

$$E_C - E_{fb} = kT \ln N_C/N_D \quad (7.6)$$

$$(E - E_{fb}) = -e(V - V_{fb}) \quad (7.7)$$

Using the above equation, the difference between Fermi level and edges of conduction band ( $E_C - E_F$ ) for  $\text{MoSe}_x\text{Te}_{2-x}$  have been obtained and are given in Table 7.1. By subtracting the band gap energy, as obtained for  $\text{MoSe}_x\text{Te}_{2-x}$  crystals given in Table 7.1. from the values of  $E_C$ , conduction valence band positions were located as depicted in Fig. 7.4. Figure 7.4 suggests that the redox potential ( $V_{\text{redox}}$ ) within gap, positive of  $-0.50$  V and negative of  $+0.9$  V Vs SCE should be appropriate for PEC cells of  $\text{MoSe}_x\text{Te}_{2-x}$  electrodes.

#### 7.4 Conclusion

The direct band gap of the grown series increases from  $1.1$  eV to  $1.4$  eV with increasing selenium content. The flat band potentials show an increasing trend in their value from selenides to tellurides of molybdenum.  $\text{MoSe}_x\text{Te}_{2-x}$  ( $0 \leq x \leq 2$ ) electrodes have been characterized in terms of energetic location of valence and conduction band

positions, which suggest that the redox potential within the gap, positive of  $-0.5$  V and negative of  $+0.9$  V Vs SCE should be appropriate for PEC solar cells of  $\text{MoSe}_x\text{Te}_{2-x}$  single crystals.

REFERENCES

1. Loferski, J. J. (1956)  
J. Appl. Phys. 27, 777.
2. Noufi, R. and Warren, F. (1980)  
SPIE, Vol. 248, Role of Electro-Optics  
in Photovoltaic Energy Conversion.
3. Butler, M. A. and Ginley, D. S. (1980)  
J. Mat. Sci. 15, 1.
4. Sinha, A. P. B. (1983)  
Energy Digest. Vol. 1, 1.
5. Tributsch, H. (1977)  
Ber. Bunsenges. Phys. Chem. 81, 361.
6. Noufi, R., Kohl, P. and Bard, A. J. (1978)  
J. Electrochem. Soc. 125, 375.
7. Hodes, G. (1980)  
J. Electrochem. Soc. 127, 2252.
8. Redon, A. M. and Vigneron, J. (1980)  
J. Electrochem. Soc. 127, 2347.

9. Karas, B. R. and Ellis, A. B. (1980)  
J. Am. Chem. Soc. 102, 968.
10. Sridevi, D. and Reddy, K. V. (1985)  
Mat. Res. Bull. 20, 8, 929.
11. Lemasson, P., Etcheberry, A. and  
Goutron, J. (1983)  
Electrochimica Acta 27, 3, 607.
12. Redon, A. M. and Vigneron, J. (1981)  
Solar Cells 3, 179.
13. Kautek, W. and Gerischer, H. (1980)  
Ber. Bunsenges. Phys. Chem. 84, 645.
14. Wilson, J. A. and Yoffe, A. D. (1969)  
Adv. Phys. 18, 193.

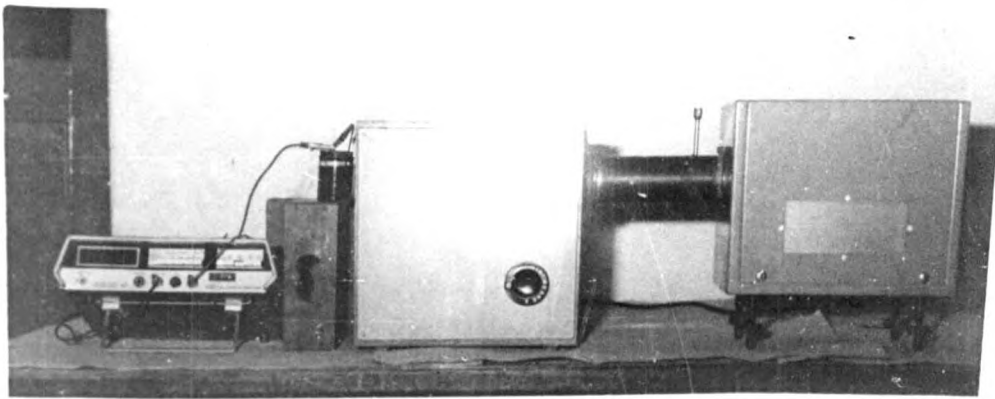


Fig. 7.1 Photograph of experimental set up for spectral response measurements.

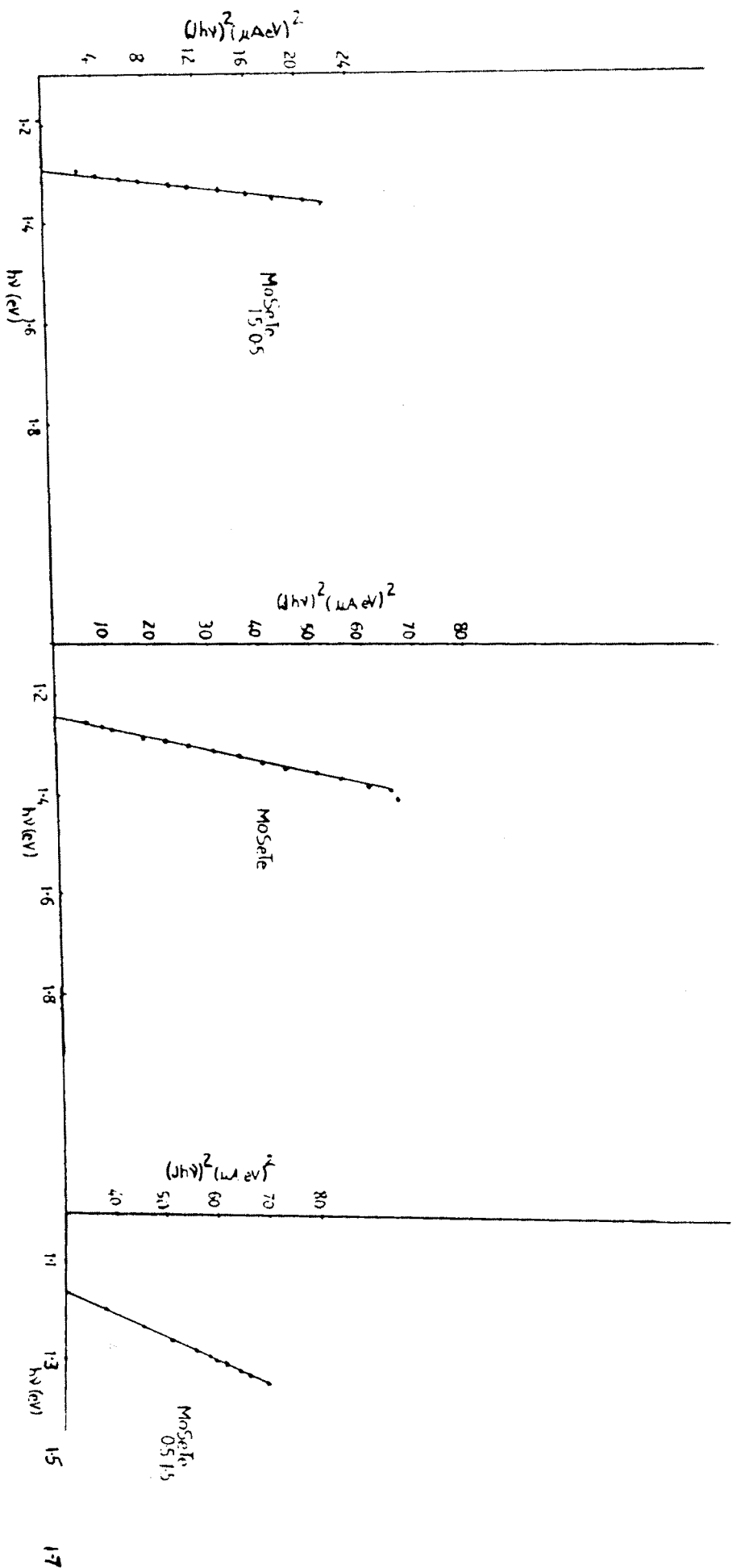


Fig. 7.2 Plots of  $(Jh\nu)^2$  versus  $h\nu$  for MoSe<sub>1.5</sub>Te<sub>0.5</sub>, MoSeTe and MoSeTe<sub>0.5</sub>Te<sub>1.5</sub>

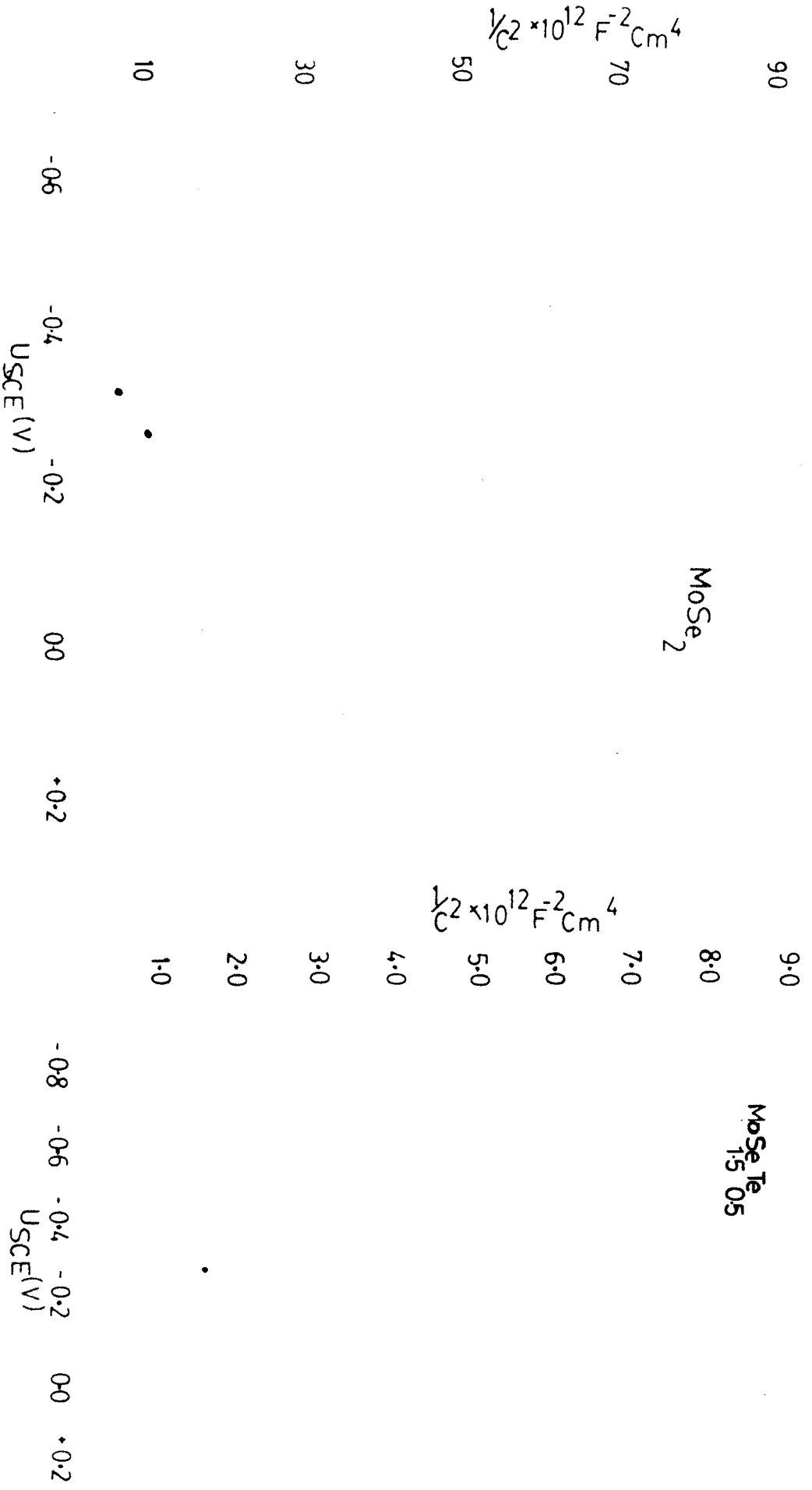


Fig. 7.3(a) Mott-Schottky Plots of MoSe<sub>2</sub> and MoSe<sub>1.5</sub>Te<sub>0.5</sub>



22

1:1

—MoSeTe  
0.5:1.5

18

0:9

MoSeTe

—MoTe<sub>2</sub>

$C \times 10^{-14} \text{ F cm}^{-2}$

10

$\frac{1}{2} C^2 \times 10^{12} \text{ F}^{-2} \text{ cm}^{-4}$

0:7

6

0:3

2

0:1

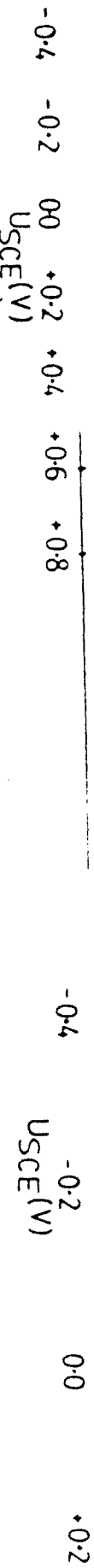


Fig. 7.3(b) Mott-Schottky Plots for MoSeTe, MoSe<sub>0.5</sub>Te<sub>1.5</sub> and MoTe<sub>2</sub>

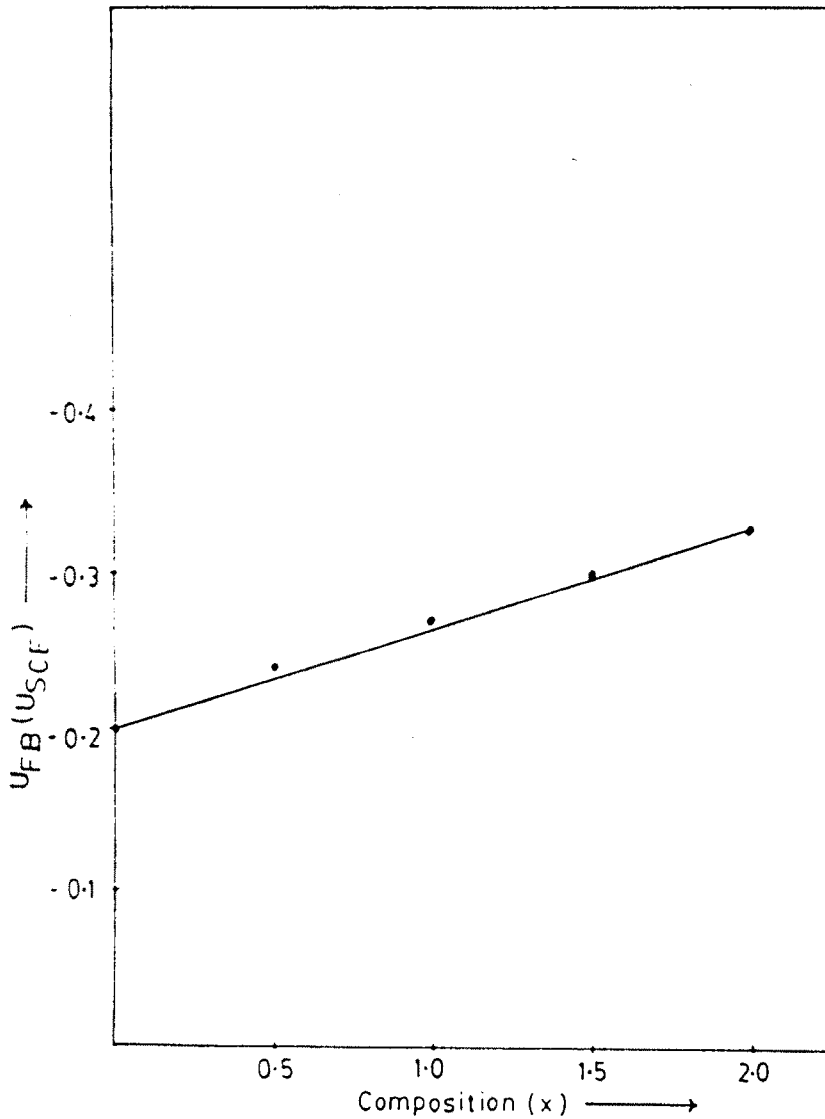


Fig. 7.4 Variation of flat band potentials with the composition 'X' of  $\text{MoSe}_x\text{Te}_{2-x}$  in aqueous iodine/iodide solutions

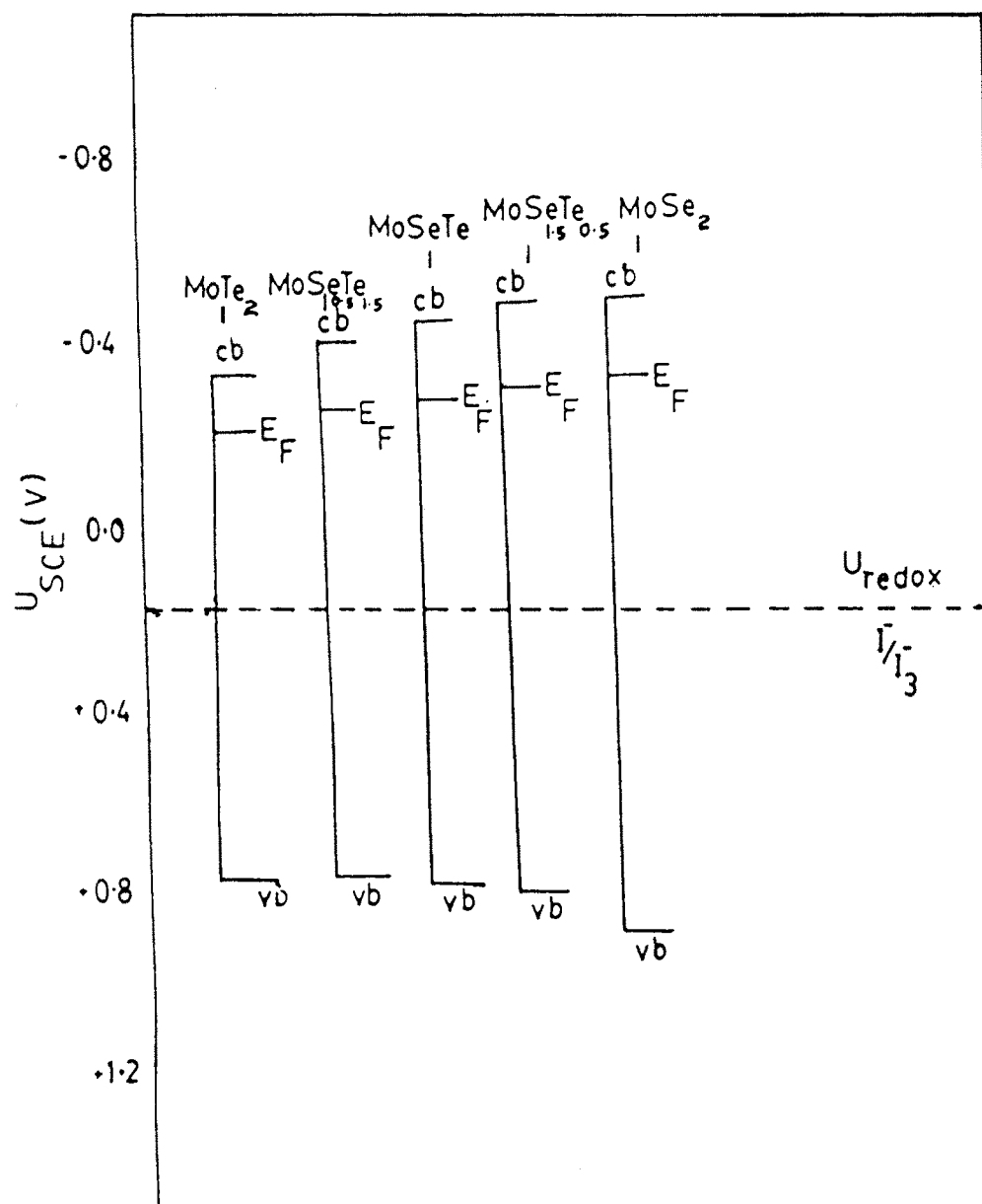


Fig. 7.5 Position of band-edges of  $\text{MoSe}_x\text{Te}_{2-x}$  in aqueous iodine/iodide solutions